Journal of Materials Chemistry C

Accepted Manuscript

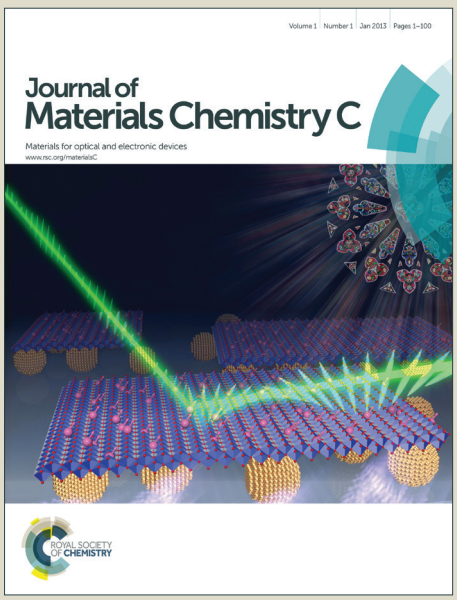

ROYAL SOCIETY OF CHEMISTRY

www.rsc.org/materialsC

An ABA Triblock Copolymer Strategy for Intrinsically Stretchable Semiconductor

Rui Peng,[a] Bo Pang,[a] Daqing Hu,[a] Mengjie Chen, [a] Guobing Zhang,[a] Xianghua Wang,[a] Hongbo Lu,[a,b] Kilwon Cho,[c] Longzhen Qiu[a,b]*

[a] Key Lab of Special Display Technology, Ministry of Education, National Engineering Lab of Special Display Technology, State Key Lab of Advanced Display Technology, Academy of Opto-Electronic Technology, Hefei University of Technology, Hefei, 230009, China. Email: lzhqiu@hfut.edu.cn

[b] Key Lab of Advanced Function Materials and Devices, Anhui Province, School of Chemical Engineering, Hefei University of Technology, Hefei, 230009, China.

[c] Department of Chemical Engineering, Pohang University of Science and Technology, Pohang, 790-784, Korea.

Abstract

A novel semiconductor-rubber-semiconductor (P3HT-PMA-P3HT) triblock copolymer has been designed and prepared according to the principle of thermoplastic elastomers. It behaves as a thermoplastic elastomer with a Young's modulus (*E*) of 6 MPa for an elongation at break of 140% and exhibits good electrical properties with a carrier mobility of 9×10^{-4} $cm^2V^{-1}s^{-1}$. This novel semiconductor may play an important role in the low-cost and large-area stretchable electronics.

Keywords:

thermoplastic elastomers, stretchable semiconductors, poly(3-hexylthiophene)

1 Introduction

Conjugated polymers have attracted enormous interest because of their potential applications in organic photovoltaics (OPVs),[1-4] organic light-emitting diodes (OLEDs),[5, 6] and organic field-effect transistors (OFETs).[7-9] Compared with their inorganic counterparts, conjugated polymers are much more flexible and suitable for fabricating revolutionary flexible electronic products which would be light in weight, bendable or foldable, and compatible to low-cost fabrication methods such as high-throughput printing processing. A large number of highly bendable polymer devices built on plastic or metal foils have been demonstrated with flexed radii as small as several millimeters.[10, 11] However, the rigid planar-conjugated backbones and highly crystallized merits of conjugated polymers will inhibit the molecular motion and make the materials stiff and brittle,[12, 13] which could lead to malfunction of the electronic devices under flexure. Furthermore, realization of stretchability in electronics is motivated by a wide range of applications including wearable electronics, smart skins, artificial organs, and integrated robotic sensors.[14-16] Such devices require materials that can sustain large mechanical strain without the loss of their function. Various techniques have been developed to modify the mechanical properties of the semiconductors, such as curvy structure,[16] nanofibrilar network[10] and microcrack.[13] Especially, Lipomi and coworkers systematically studied the effect of molecular structure including side chains,[17] segmentation on main chains[18] and additives[19] on the mechanical properties of conjugated polymers.

Conjugated block copolymers are promising molecular architectures because the physical and electrical properties of the copolymers can be fine-tuned either by changing the physical properties of the segments or by controlling the self-assembled nanostructures. Combining a conjugated polymer block with flexible insulating blocks has the potential to generate conjugated copolymers with excellent mechanical properties. There have been a large number of reports on the synthesis of block copolymers containing a conjugated segment.[20-32] For example, Muller et al.[21] reported that diblock copolymers of polyethylene (PE) and P3HT display outstanding

flexibility and toughness with elongations at break exceeding 600%. However, the P3HT-b-PE copolymers show typical plastic characteristics and irreversible deformation under strain.

(Insert Figure 1 here)

In this contribution, we conceptualize an unprecedented strategy to design and prepare semiconducting polymers with high elasticity according to the principle of ABA triblock copolymers thermoplastic elastomers (TPEs), such as polystyrene-*b*-polybutadiene-*b*-polystyrene (SBS) and polystyrene-*b*-polyisoprene-*b*-polystyrene (SIS). The elasticity of such TPEs is derived from a two-phase nanostructure comprising hard polystyrene domains acting as physical cross-links in a rubbery matrix (Figure 1a). Inspired by this system, we hypothesize that a class of novel semiconducting TPEs can be achieved by using rigid semiconducting polymer chains as hard segments and rubbery chains such as polyacrylate or poly(butadiene) as soft segments. However, charge transport in these semiconducting TPEs is challenging as the semiconducting phase disperses as minor component in the dielectric matrix and can hardly form a conducting active channel. To solve this problem, a key feature of our process is controlling the semiconducting component to form a nanofibrillar network with ordered molecular stacking embedded in the insulating polymer matrix (Figure 1b). Our previous results have shown that the embedded nanofibrillar networks permit the reduction of the semiconductor content to a level as low as 3 wt% without considerable degradation of the field-effect characteristics.[33, 34] If this architecture design indeed leads to the formation of semiconducting TPEs, it would provide a powerful platform for the preparation of a variety of semiconducting polymers with intrinsic stretchability.

2 Experimental

2.1 Materials

Diethyl meso-2,5-dibromoadipate and *N,N,N',N'',N''*- pentamethyldiethylenetriamine

(PMDETA) were obtained from TCI Co. Ltd., Shanghai, China. Other chemicals used in this work were purchased from Sigma-Aldrich Chemical Company, Sinopharm Chemical Reagent Co. Ltd., China. Methyl acrylate (MA) passed through a column of basic alumina to remove the 4-methoxyphenol stabilizer. Chemical regents were purchased and used as received. Tetrahydrofuran (THF) and toluene were freshly distilled over sodium wire under nitrogen prior to use.

2.2 Synthesis of PMA block (Br-PMA-Br) (1)

An oven-dried 100 ml flask was cooled under nitrogen-condition and charged with diethyl meso-2,5-dibromoadipate (0.58 g, 1.61 mmol), methyl acrylate (10 g, 116.3mmol), toluene (6 ml), PMDETA (0.28 g, 1.61 mmol) and a stir bar. The reaction mixture was purged with nitrogen for 30 min under ice-bath, CuBr (0.23 g, 1.61 mmol) was added. The flask was sealed with a rubber septum and warmed to room temperature. The reaction mixture was placed in an oil bath at 75 ^{o}C. After stirring the mixture for 4 h, the reaction was cooled to room temperature. The mixture was added in THF and passed through a neutral column (eluent=THF) to remove the residual catalyst. The solution was concentrated by a rotary evaporator. Afterward, it was precipitated into cold methanol to remove the residual monomer and other impurities. The polymer was dried under vacuum at 50 ^{o}C for 24h. (8.6 g, 86% yield). Data for PMA_{128}: GPC: $\overline{Mn}$ =11.2 kDa, PDI=1.08. ^{1}HNMR (Figure S1 in Electronic Supporting Information, $CDCl_3$, ppm): δ 4.25 (m, C*H*-Br), 4.13 (broad, OCH_2CH_3), 3.76 (m, $CHBrCOOCH_3$), 3.69 (s, CH_3O), 2.3 (broad, C*H* of polymer backbone), 1.94, 1.67, 1.51 (m, CH_2 of polymer backbone), 1.25 (t, OCH_2CH_3). FT-IR: $\upsilon_{c=o}$ =1750cm^{-1}.

2.3 Synthesis of PMA block (N_3-PMA-N_3) (2)

A round-bottomed glass flask (100 ml) with a magnetic bar was charged with Br-PMA-Br ($\overline{Mn}$ =11.2 KDa. 5 g, 0.45 mmol), NaN_3 (0.29 g, 4.5 mmol), DMF (40 ml). The resulting solution was stirred at room temperature for 24 h. After adding CH_2Cl_2 (200ml) and water (200 ml), the organic phase was separated and washed with

water (30 ml×4), and then dried by Na_2SO_4. The solution was concentrated by a rotary evaporator. Afterward, it was precipitated into cold methanol to remove the residual DMF. The polymer was dried under vacuum at 50 ^oC for 24 h. (4 g, 80% yield). GPC: $\overline{Mn}$ =11.2 KDa, PDI= 1.08. ^{1}HNMR (Figure S2 in Electronic Supporting Information, $CDCl_3$, ppm): δ 4.13 (broad, OCH_2CH_3), 3.93 (CH_2-N_3), 3.76 (m, $CHN_3COOCH3$), 3.69 (s, CH_3O), 3.66 (broad, CH_3 of polymer backbone), 2.3 (broad, CH of polymer backbone), 1.94, 1.67, 1.51 (m, CH_2 of polymer backbone), 1.25 (t, OCH_2CH_3). FT-IR: $\upsilon_{c=o}$ =1750 cm^{-1}. υ_{N3} =2100 cm^{-1}.

2.4 Synthesis of Ethynyl-Terminated P3HT (P3HT-Ethynyl) (3)

According to the literature,[20, 23] in a typical experiment, an oven-dried two-neck glass flask (200 ml) was cooled under nitrogen-condition and charged with 2,5-dibromo-3-hexylthiophene (4.36 g, 13.4 mmol), anhydrous THF (40 ml) and a magnetic stir bar. After adding tert-Butylmagnesium chloride (13,4 ml, 1M solution in THF), the reaction mixture was stirring at room temperature for 2 h. Subsequently, the mixture was diluted to 130 ml with anhydrous THF and Ni(dppp)Cl_2 (0.069 g, 0.127 mmol) was added. After 30 min, ethynylmagnesium bromide (2.5ml, 0.5M solution in THF) was added. After an additional 30 min, methanol was poured in the glass flask, which causes a dark-pure solid to precipitate. The desired P3HT was purified by a series of precipitation and dried under vacuum at room temperature. (1.7 g, 40% yield).GPC: $\overline{Mn}$ =5.6 KDa, PDI= 1.02. ^{1}HNMR (Figure S3 in Electronic Supporting Information, $CDCl_3$, ppm): δ 6.98 (s, CH of the thiophene ring), 3.52 (s, CH of terminal ethynyl), 2.80 (t, $CH_2CH_2CH_2CH_2CH_2CH_3$), 1.71 (m, $CH_2CH_2CH_2CH_2CH_2CH_3$), 1.50-1.30 (m, $CH_2CH_2CH_2CH_2CH_2CH_3$), 0.9 (t, $CH_2CH_2CH_2CH_2CH_2CH_3$).

2.5 Synthesis of P3HT-PMA-P3HT Triblock Copolymer (4)

N_3-PMA-N_3 ($\overline{Mn}$ =11.2 KDa, 0.5 g, 0.0455 mmol), P3HT-Ethynyl ($\overline{Mn}$ =5.6KDa, 0.51 g, 0.0910 mmol), PMDETA (0.016 g, 0.0910 mmol) were dissolved in the

anhydrous THF. The resulting solution was purged with nitrogen for 40 min under ice-bath, Subsequently, CuBr (0.014g, 0.0910 mmol) was added under nitrogen-condition. The reaction mixture was placed in an oil bath at 50 ^{o}C for 3 days and taken out of oil bath to cool to room temperature. The solution was diluted with THF and passed through a neutral column (eluent=THF) to remove residual catalyst, concentrated by a rotary evaporator to afford the crude product. The desired polymers were confirmed by HNMR and GPC. GPC: $\overline{Mn}$ =19 KDa, PDI=1.12. ^{1}HNMR ($CDCl_3$, ppm): 7.43 (s, C*H* of triazole rings), 6.98 (s, C*H* of the thiophene ring), 4.13 (broad, O$CH_2$$CH_3$), 3.66 (broad, O$CH_3$), 2.80 (t, $CH_2CH_2CH_2CH_2CH_2CH_3$), 2.3 (broad, C*H* of poly(methyl acrylate) block), 1.94 (broad , CH_2CH of poly(methyl acrylate) block), 1.71 (m, $CH_2CH_2CH_2CH_2CH_2CH_3$), 1.50-1.30(m, $CH_2CH_2CH_2CH_2CH_2CH_3$).

2.6 Fabrication and Characterization of Field-Effect Transistors

Heavily n-doped Si wafer with 300 nm thermally grown SiO_2 surface layer (capacitance of 10.8 nFcm^{-2}) was employed as the substrate for the fabrication of OFETs. The n-type Si wafer serves as common gate electrode and the SiO_2 layer acts as gate dielectric. Prior to the modification of the SiO_2 layer with octadecyltrichlorosilane (ODTS), the wafer was cleaned in piranha solution (70 vol % H_2SO_4 + 30 vol % H_2O_2) for 30 min at 100 ^{o}C and washed with copious amounts of distilled water. The ODTS self-assembled monolayers (SAMs) were prepared by dipping the cleaned wafer in a 0.1 M toluene solution of ODTS for 2 h. A chloroform solution containing semiconductor polymer was dropped onto the ODTS-SAM modified wafer and spin-coated. The polymer films were subsequently annealed (100-200 ^{o}C) in nitrogen. Then Au source-drain electrodes were prepared by thermal evaporation. The OFETs devices had a channel length (L) of 100 μm and channel width (W) of 1 mm. The electrical characteristics of the OFET devices were measured in accumulation mode using Keithley 2400 under ambient conditions. The mobility were obtained by the following equation used at saturation regime: $I_d = (W/2L)C_i\mu(V_g-V_{th})^2$, where W/L is the channel width/length, I_d is the drain current in the

saturated regime, C_i is the capacitance of SiO_2 gate-dielectric, and V_{th} is the threshold voltage.

2.7 Instrumentation

Nuclear magnetic resonance (NMR) spectra were recorded on a Mercury plus 600 MHz machine. Gel permeation chromatography (GPC) analyses were performed on a Waters Series 1525 gel coupled with UV-vis detector using tetrahydrofuran as eluent with polystyrene as standards, Polystyrene standards in the range of 4100 to 278000 g/mol were used to calibrate the GPC. The flow rate for the GPC system is 1 mL/min. Differential scanning calorimetry (DSC) was performed on a TA instrument Q2000 in a nitrogen atmosphere. The sample (about 3.0 mg in weight) was first heated up to 250 ^{o}C and held for 5 min to remove thermal history, followed by the cooling rate of 10 ^{o}C/min to -40 ^{o}C and then heating rate of 10 ^{o}C/min to 250 ^{o}C in all cases. UV-vis absorption spectra were recorded on a Perkin Elmer model λ 20 UV-vis spectrophotometer. IR spectra were recorded using Thermo Nicolet Spectrum Nicolet 67 system using KBr pellets. Atomic force microscopy (AFM) was obtained using a Veeco Multimode V instrument. Tensile tests were performed at room temperature on rectangular sample (20mm×5mm×1mm) using a CMT4000 tensile machine, with a strain rate 2mm/min.

3 Results and discussion

(Insert Scheme 1 here)

3.1 Synthesis and Characterization: The synthetic routes for triblock copolymers were illustrated in Scheme 1. A novel semiconductor-rubber-semiconductor triblock copolymer, poly(3-hexylthiophene)-poly(methylacrylate)-poly(3-hexylthiophene) (P3HT-PMA-P3HT), was synthesized via the "click" reaction of two ethynyl-terminated P3HT (P3HT–C≡CH) chains and a α, ω-diazido-terminated poly(methyl acrylate) (N_3–PMA–N_3). Well-fined N_3–PMA–N_3 was synthesized via Cu-mediated atom transfer radical polymerization of methyl acrylate initiated by diethyl meso-2, 5-dibromoadipate, followed by displacement of the bromide

end-group with azides using NaN_3 in DMF at room temperature. Monomodal P3HT–C≡CH was prepared via a Ni-catalyzed Grignard metathesis (GRIM) polymerization and purified according to literature procedures.[35] N_3–PMA–N_3 was reacted with 2 equiv of P3HT–C ≡ CH using N,N,N`,N``,N``-pentamethyldiethylenetriamine (PMDETA)/CuBr as the catalyst system at 40 °C in tetrahydrofuran (THF). After filtering the resulting reaction mixture through neutral alumina to remove the catalyst, the crude P3HT-PMA-P3HT triblock copolymers were obtained by precipitating the reaction mixtures in methanol.

(Insert Figure 2 here)

(Insert Figure 3 here)

In **Figure 2**, the ^{1}H-NMR spectra determined the structure of triblock copolymers. The absence of the starting P3HT–C≡CH and N_3–PMA–N_3 was confirmed by the disappearance of both resonances corresponding to the alkynyl groups at δ = 3.52 ppm and the azide moiety at δ = 3.9 ppm. The formation of the triazole rings was confirmed by the presence of a new resonance at δ = 7.43 ppm[20] and the disappearance of the diagnostic υ_{N3} IR signal (Figure S4 in Electronic Supporting Information). Moreover, after purification via gel permeation chromatography (GPC), a triblock copolymer composed of two rodlike 5600g/mol rr-P3HT chains covalently linked to a 11200g/mol PMA coil polymer with an overall number-average molecular weight of 19000g/mol was obtained (see in Figure 3 a, b). Notably, a small shoulder appeared in the GPC trace of the crude triblock copolymers since P3HT with alkyne end group could not reach 100% conversion.[36, 37] However, the limited portion of P3HT homopolymer in triblock copolymer has no influence on the electrical performance and mechanics, because P3HT can self-assemble into well-ordered nanowire acting as a charge transport channel. The chemical composition of the four triblock copolymers derived from P3HT and PMA segments of different molecular weights are summarized **in Table 1.**

(Insert Table 1 here)

(Insert Figure 4 here)

3.2 Optical Properties: UV-visible absorbance spectra, which were referred to the extended triblock and collapsed triblock were collected in dilute chloroform solution and solid state films. In Figure 4 (red line), the triblock exhibited a broad absorption peak centered at 455 nm, which corresponded to the π-π* electronic transition of triblock copolymer in solution. This phenomenon resembled the characteristic of highly rr-P3HT. The black line represents the collapsed triblock, a broad π-π* electronic transition band was evident with a peak centered at 518 nm and two addition vibronic structures at 548 nm and 605 nm which were interpreted as the coupling of the C=C double bond symmetric stretch and the π-π* electronic transition. The large red shift (about 70 nm) between solution and solid state films indicated the presence of strong intermolecular interaction and the planarization effect of conjugated polymer backbone. The results suggest that intermolecular interactions are relatively strong in favor of the mobility.

(Insert Figure 5 here)

3.3 Thermal and Mechanical Properties: The thermal behavior of the P3HT-*b*-PMA-*b*-P3HT triblock copolymer was investigated by differential scanning calorimetry (DSC) (Figure 5). The DSC trace of P3HT-*b*-PMA-*b*-P3HT triblock copolymer was typical of an immiscible system**.** The result was in agreement with the obvious difference in solubility between the P3HT (13.1 (MPa)1/2)[38] and the PMA (20.7 (MPa)1/2)[39], which provides a strong driving force for phase separation. It showed a glass transition at 2 °C corresponding to the T_g of PMA phase and an endotherm peak at 200°C corresponding to T_m of P3HT phase. The T_g of PMA segments and the T_m of P3HT segments in triblock copolymer were lower than that of PMA (10 °C)[40] and P3HT (215.6 °C)[41] homopolymers because of their relatively low molecular weight.

(Insert Figure 6 here)

Although the starting N_3–PMA–N_3 is viscous and P3HT–C≡CH is brittle at room

temperature, the P3HT-*b*-PMA-*b*-P3HT triblock copolymers have excellent mechanical properties. The film of **P4** can be elastically deformed as displayed in the insert of Figure 6. The strain-stress curve indicates a Young's modulus (E) of 6 MPa, an elongation at break (ε) of 140% and a true stress at break [$\sigma_t = \sigma(1 + \varepsilon/100)$] (here, σ is the maximum stress at break) of 1.4 MPa, respectively. Compared with the E of 28 MPa, ε of 13% and σ_t of 4 MPa for the P3HT homopolymer reported in the literature,[21] the modulus became lower and the elongation became larger which are typical characteristics of plastic-to-rubber transition. It should be noted that the mechanical properties of P3HT are highly dependent on measuring method. For instance, O'Connor[12] and Lipomi[42] reported the modulus of P3HT films was 0.25 GPa and 0.92 GPa using a buckling-based metrology. The reason may be the buckling-based technique measured the in-plane elastic modulus, and the anisotropic microstructure of the films may lead to an anisotropic elastic modulus. For comparison, we used the data of bulk samples obtained from a similar measurement technique. Furthermore, the mechanical properties of our triblock copolymer could be improved by increasing the molecular weight of the soft PMA block.

(Insert Figure 7 here)

3.4 The Film Morphologies and Microstructure: Film morphology and crystallinity played an important role for OFETs device performance. Atomic force microscopy (AFM) was applied to investigate the morphology of **P4** film annealed at different temperatures for 15 min (Figure 7). The AFM phase image of as-prepared film without any thermal annealing shows a granular phase pattern. As the annealing temperature increased, the granular domain is elongated. When annealing at 200 °C, the AFM images showed clear evidence of nanofibrillar structures with a length of several hundreds of nanometers and a width about 10 nm. Considering the PMA is in a rubbery state, the nanofibrillar structures can be attributed to the result of π—π stacking of P3HT segments. The P3HT nanofibers with high aspect ratios can keep the connectivity of the semiconducting layers in the block copolymer films and thus plays significant role in achieving effective charge transport.[43]

(Insert Figure 8 here)

3.5 OFETs Characterization: OFET device with bottom-gate and top-contact geometry were used to investigate the field-effect mobility of P3HT-*b*-PMA-*b*-P3HT triblock copolymers. Figures 8 shows the typical field-effect transistor characteristics of **P4** measured in the accumulation mode under ambient conditions. The devices displayed well-behaved p-type transistors with a clear linear regime at small source-drain voltages and a saturation regime at V_{DS} values higher than the gate voltage. Table 2 summarizes the device parameters for all of the polymers. The homo P3HT films with molecular weight of 3.8 and 6.6 kg/mol (NMR) showed carrier mobilities of 1.7×10^{-4} and 2.4×10^{-4} $cm^2V^{-1}s^{-1}$ (Figure S5 in Electronic Supporting Information), respectively. This poor mobilities observed in our work attributed to the low molecular weight of P3HT and are comparable with those of P3HT with similar molecular weight reported in literature.[37] The field-effect performances of triblock copolymers are highly dependent on the content of P3HT segments. The **P1** (41 % P3HT) and **P3** (55% P3HT) with relatively high content of P3HT displayed enhanced mobilities of 3.5×10^{-4} and 3.0×10^{-4} $cm^2V^{-1}s^{-1}$ compared to their P3HT homopolymers. The enhancement of charge transport properties was also reported in poly(3-hexylthiophene)-*b*-polystyrene diblock copolymers and was ascribed to the highly crystalline, ordered P3HT domains in the copolymer films.[43] The mobility of the triblock copolymers decreased with higher PMA content because the PMA segment is an insulator. The maximum carrier mobility was 9×10^{-4} $cm^2V^{-1}s^{-1}$ for the **P3** film.

(Insert Table 2 here)

(Insert Figure 9 here)

The change of electrical properties of P4 film under stress was evaluated using a transfer process as illustrated in Figure 9a. The P4 film was firstly spin coated onto a PDMS substrate and followed by straining to a certain elongation. Then the film was transfer to a silicon substrate with pre-defined source and drain electrodes at the

tensile state. Figure 9b shows the change of mobility as a function of strain. The on-current slowly decrease up to elongation of 20%. After that, a considerable decrease was observed with the elongation range from 40% to 60%. Though the mobility monotonously decreased as the elongation increased, the film with 60% elongation still showed field-effect performance and the mobility is 10% of the film without any strain. Figure 9d shows the change in transfer curves measured in a stretch cycles at strain of 40%. When the P4 sample was stretched to 40% and released back to 0%, the on-current irreversibly decrease to about 50% of the pristine state. This decrease may be caused by the non-optimized phase structure of the films. Further study will be conducted to improve it.

4 Conclusions

In conclusion, novel copolymers based on amorphous PMA block and two crystalline P3HT block were successfully synthesized via coupling of the alkyne-terminated P3HT with the diazide-terminated PMA using a click reaction. These triblock copolymers behaved as a thermoplastic elastomer with a Young's modulus (*E*) of 6 MPa for an elongation at break of 140%. The spin-cast triblock copolymer films were found to self-assemble into well ordered nanofibrillar structure under thermal annealing, which is optimal for charge transfer in field-effect transistors. A maximum saturated hole mobility of 9×10^{-4} $cm^2V^{-1}s^{-1}$ was obtained for P3HT-*b*-PMA-*b*-P3HT triblock copolymer containing 55 wt% P3HT. The structure of semiconductor-rubber-semiconductor (SRS) would have a significant impact on the next generation of stretchable electronics.

Acknowledgement

This research was supported by National Basic Research Program of China (Grant No. 2012CB723406), National Natural Science Foundation of China (Grand No. 61107014, 51203039, 21204017, 21174036, 51103034), Program for New Century Excellent Talents in University (Grant No. NCET-12-0839)

Notes and references

1. J. B. You, L. T. Dou, K. Yoshimura, T. Kato, K. Ohya, T. Moriarty, K. Emery, C. C. Chen, J. Gao, G. Li and Y. Yang, *Nat. Commun*, 2013, **4**.
2. H. X. Zhou, L. Q. Yang and W. You, *Macromolecules*, 2012, **45**, 607.
3. H. L. Yip and A. K. Y. Jen, *Energy Environ. Sci.*, 2012, **5**, 5994.
4. J. W. Chen and Y. Cao, *Acc. Chem. Res.*, 2009, **42**, 1709.
5. M. C. Gather, A. Kohnen and K. Meerholz, *Adv. Mater.*, 2011, **23**, 233.
6. S. Reineke, F. Lindner, G. Schwartz, N. Seidler, K. Walzer, B. Lussem and K. Leo, *Nature*, 2009, **459**, 234.
7. T. Lei, J.-H. Dou, X.-Y. Cao, J.-Y. Wang and J. Pei, *J. Am. Chem. Soc.*, 2013, **135**, 12168.
8. P. Sonar, T. R. B. Foong, S. P. Singh, Y. Li and A. Dodabalapur, *Chem. Commun.*, 2012, **48**, 8383.
9. J. Li, Y. Zhao, H. S. Tan, Y. Guo, C.-A. Di, G. Yu, Y. Liu, M. Lin, S. H. Lim, Y. Zhou, H. Su and B. S. Ong, *Sci. Rep*, 2012, **2**, 754.
10. M. Kaltenbrunner, T. Sekitani, J. Reeder, T. Yokota, K. Kuribara, T. Tokuhara, M. Drack, R. Schwodiauer, I. Graz, S. Bauer-Gogonea, S. Bauer and T. Someya, *Nature*, 2013, **499**, 458.
11. G. H. Gelinck, H. E. A. Huitema, E. Van Veenendaal, E. Cantatore, L. Schrijnemakers, J. Van der Putten, T. C. T. Geuns, M. Beenhakkers, J. B. Giesbers, B. H. Huisman, E. J. Meijer, E. M. Benito, F. J. Touwslager, A. W. Marsman, B. J. E. Van Rens and D. M. De Leeuw, *Nat. Mater.*, 2004, **3**, 106.
12. B. O'Connor, E. P. Chan, C. Chan, B. R. Conrad, L. J. Richter, R. J. Kline, M. Heeney, I. McCulloch, C. L. Soles and D. M. DeLongchamp, *Acs Nano*, 2010, **4**, 7538.
13. A. Chortos, J. Lim, J.W.F. To, M. Vosgueritchian, T.J. Dusseault, T.-H. Kim, S. Hwang, Z. Bao, *Adv. Mater.*, 2014, **26,** 4253.
14. D. J. Lipomi, M. Vosgueritchian, B. C. K. Tee, S. L. Hellstrom, J. A. Lee, C. H. Fox and Z. N. Bao, *Nat. Nanotechnol.*, 2011, **6**, 788.
15. T. Sekitani, H. Nakajima, H. Maeda, T. Fukushima, T. Aida, K. Hata and T. Someya, *Nat. Mater.*, 2009, **8**, 494.
16. D. Y. Khang, H. Q. Jiang, Y. Huang and J. A. Rogers, *Science*, 2006, **311**, 208.
17. D.J. Lipomi, H. Chong, M. Vosgueritchian, J. Mei, Z. Bao, *Sol. Energ. Mat. Sol. C.,* 2012, **107,** 355.

18. S. Savagatrup, A.S. Makaram, D.J. Burke, D.J. Lipomi, *Adv. Funct. Mater.,* 2014, **24**, 1169.

19. A.D. Printz, S. Savagatrup, D.J. Burke, T.N. Purdy, D.J. Lipomi, *Rsc Adv.,* 2014, **4,** 13635.

20. M. Urien, H. Erothu, E. Cloutet, R. C. Hiorns, L. Vignau and H. Cramail, *Macromolecules*, 2008, **41**, 7033.

21. C. Muller, S. Goffri, D. W. Breiby, J. W. Andreasen, H. D. Chanzy, R. A. J. Janssen, M. M. Nielsen, C. P. Radano, H. Sirringhaus, P. Smith and N. Stingelin-Stutzmann, *Adv. Funct. Mater.*, 2007, **17**, 2674.

22. R. Duan, L. Ye, X. Guo, Y. Huang, P. Wang, S. Zhang, J. Zhang, L. Huo and J. Hou, *Macromolecules*, 2012, **45**, 3032.

23. Z. Q. Wu, R. J. Ono, Z. Chen and C. W. Bielawski, *J. Am. Chem. Soc.*, 2010, **132**, 14000.

24. H. C. Moon, A. Anthonysamy, Y. Lee and J. K. Kim, *Macromolecules*, 2010, **43**, 1747.

25. Q. Zhang, A. Cirpan, T. P. Russell and T. Emrick, *Macromolecules*, 2009, **42**, 1079.

26. S. P. Wu, L. J. Bu, L. Huang, X. H. Yu, Y. C. Han, Y. H. Geng and F. S. Wang, *Polymer*, 2009, **50**, 6245.

27. C.-A. Dai, W.-C. Yen, Y.-H. Lee, C.-C. Ho and W.-F. Su, *J. Am. Chem. Soc.*, 2007, **129**, 11036.

28. J. Liu, E. Sheina, T. Kowalewski and R. D. McCullough, *Angew. Chem. Int. Ed.*, 2002, **41**, 329.

29. M. C. Stefan, M. P. Bhatt, P. Sista and H. D. Magurudeniya, *Polym. Chem.*, 2012, **3**, 1693.

30. M. C. Iovu, M. Jeffries-El, E. E. Sheina, J. R. Cooper and R. D. McCullough, *Polymer*, 2005, **46**, 8582.

31. M. Sommer, A. S. Lang and M. Thelakkat, *Angew. Chem. Int. Ed.*, 2008, **47**, 7901.

32. K. Palaniappan, N. Hundt, P. Sista, H. Nguyen, J. Hao, M. P. Bhatt, Y. Y. Han, E. A. Schmiedel, E. E. Sheina and M. C. Biewer, *J. Polym. Sci., Part A: Polym. Chem.*, 2011, **49**, 1802.

33. L. Z. Qiu, X. Wang, W. H. Lee, J. A. Lim, J. S. Kim, D. Kwak and K. Cho, *Chem. Mater.*, 2009, **21**, 4380.

34. G. H. Lu, H. W. Tang, Y. P. Qu, L. G. Li and X. N. Yang, *Macromolecules*, 2007, **40**, 6579.

35. Z. Li, R. J. Ono, Z.-Q. Wu and C. W. Bielawski, *Chem. Commun.*, 2011, **47**, 197.

36. R. H. Lohwasser and M. Thelakkat, *Macromolecules*, 2012, **45**, 3070.

37. R. J. Kline, M. D. McGehee, E. N. Kadnikova, J. S. Liu, J. M. J. Frechet and M. F. Toney, *Macromolecules*, 2005, **38**, 3312.

38. J. Jaczewska, I. Raptis, A. Budkowski, D. Goustouridis, J. Raczkowska, A. Sanopoulou, E. Pamula, A. Bernasik and J. Rysz, *Synth. Met.*, 2007, **157**, 726.

39. J. E. Mark, Physical Properties of Polymer Handbook (2nd edition), Springer, New York, 2007.

40. I. Brandrup, E. H. Immergut and E. A. Grulke, eds., *Polymer Handbook, 4th ed.*, John Wiley & Sons, New York, 1999.

41. H. C. Yang, T. J. Shin, L. Yang, K. Cho, C. Y. Ryu and Z. N. Bao, *Adv. Funct. Mater.*, 2005, **15**, 671.

42. S. Savagatrup, E. Chan, S.M. Renteria-Garcia, A.D. Printz, A.V. Zaretski, T.F. O'Connor, D. Rodriquez, E. Valle, D.J. Lipomi, *Adv. Funct. Mater.,* 2015, **25 ,** 427.

43. X. Yu, K. Xiao, J. H. Chen, N. V. Lavrik, K. L. Hong, B. G. Sumpter and D. B. Geohegan, *Acs Nano*, 2011, **5**, 3559.

Figure Captions

Figure 1. Schematic illustration of (a) the structure of SBS, (b) the structure of P3HT-b-PMA-b-P3HT triblock copolymer.

Scheme 1. Synthetic route for P3HT-*b*-PMA-*b*-P3HT triblock copolymer.

Figure 2. The HNMR spectrum of P3HT-*b*-PMA-*b*-P3HT triblock copolymer.

Figure 3. Representative GPC trace of the crude product (a, blue line) and highly purified triblock copolymers (b, blue line), poly(methylacrylate) homopolymer (b, black line) and P3HT homopolymer (b, red line).

Figure 4. UV-vis absorption spectra of P3HT-*b*-PMA-*b*-P3HT in chloroform solution and in a thin film.

Figure 5. The DSC trace of P3HT-PMA-P3HT triblock copolymer.

Figure 6. The strain─stress profile of P3HT-PMA-P3HT triblock copolymer.

Figure 7. AFM topography images (a-d) of P3HT-PMA-P3HT at different annealing temperature.

Figure 8. Field-effect characteristics of a top contact OFETs based on P4. (a) Output, and (b) transfer.

Figure 9. (a) Schematic illustration of the steps used to measure the mobility under stress. (b) Change of the transfer curves at different strains. (c) The corresponding change of mobility as a function of strains. (d) Change of the transfer curves during a stretching cycle at strain of 40%.

Table 1. Composition of P3HT-*b*-PMA-*b*-P3HT

Polymer	P3HT block (NMR)	PMA block (NMR)	P3HT (wt%)	P3HT block (GPC)	PMA block (GPC)	$\overline{Mn}$ (GPC)	PDI (GPC)
$P3HT_1$	3800	/	100	5200	/	/	1.04
$P3HT_2$	6600	/	100	5600	/	/	1.02
P1	3800	11000	41	5200	11200	19000	1.29/1.12*
P2	3800	24000	24	5200	14000	26000	1.38
P3	6600	11000	55	5600	11200	16000	1.51
P4	6600	24000	35	5600	14000	27000	1.64

* The PDI of sampled purified by GPC.

Table 2. Summary of all field-effect mobilities of rr-P3HT and the triblock copolymers

Polymer	Mobility (cm^2/Vs)	Max Mobility (cm^2/Vs)	On/off ratio	Threshold voltage
$P3HT_1$	1.5×10^{-4}	4.2×10^{-4}	33	17.6
$P3HT_2$	2.4×10^{-4}	4.5×10^{-4}	207	17.3
P1	3.5×10^{-4}	4.3×10^{-4}	166	4.9
P2	9.9×10^{-5}	1.1×10^{-4}	175	7.2
P3	3.0×10^{-4}	9.0×10^{-4}	246	-10.7
P4	1.7×10^{-4}	2.1×10^{-4}	666	-8.6

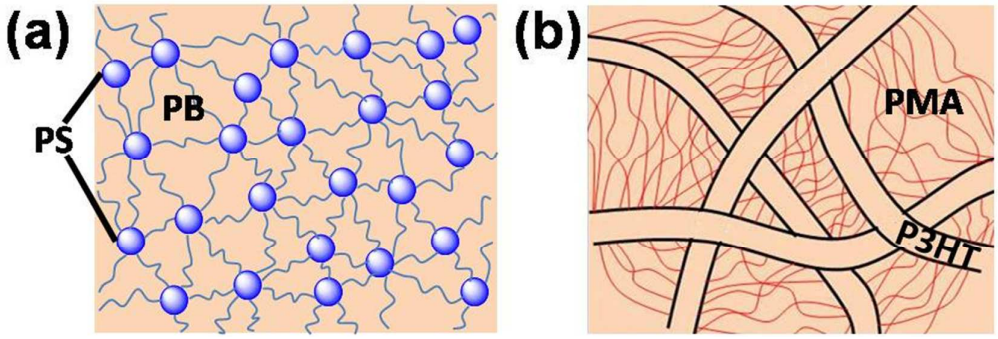

Figure 1. Schematic illustration of (a) the structure of SBS, (b) the structure of P3HT-*b*-PMA-*b*-P3HT triblock copolymer.

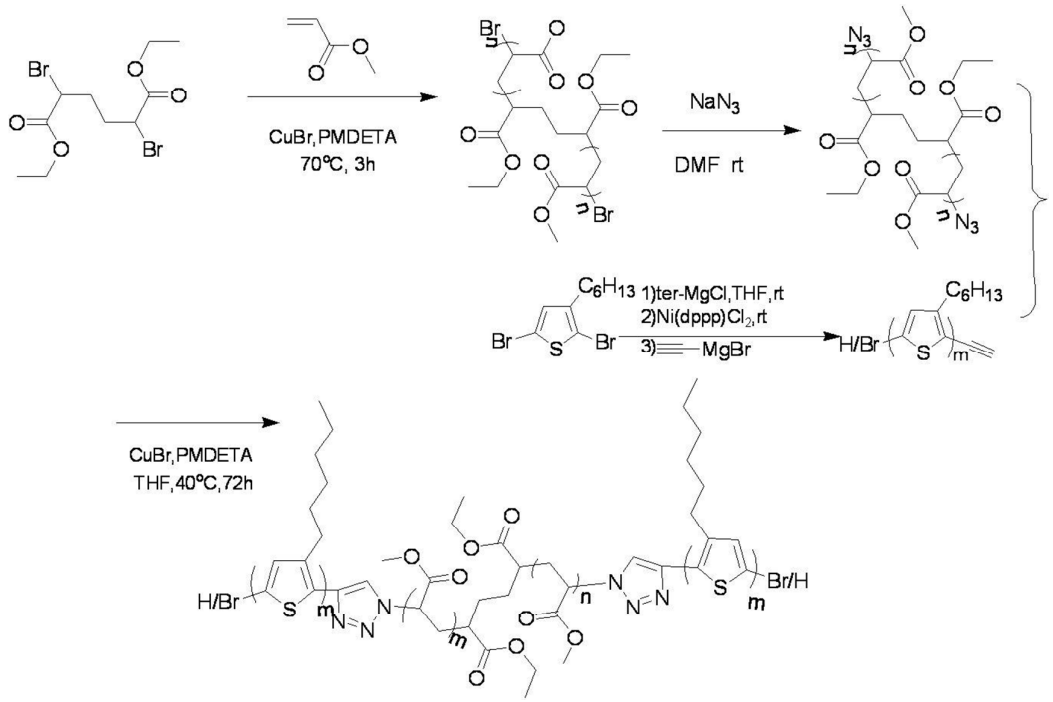

Scheme 1. Synthetic rout for P3HT-*b*-PMA-*b*-P3HT triblock copolymer.

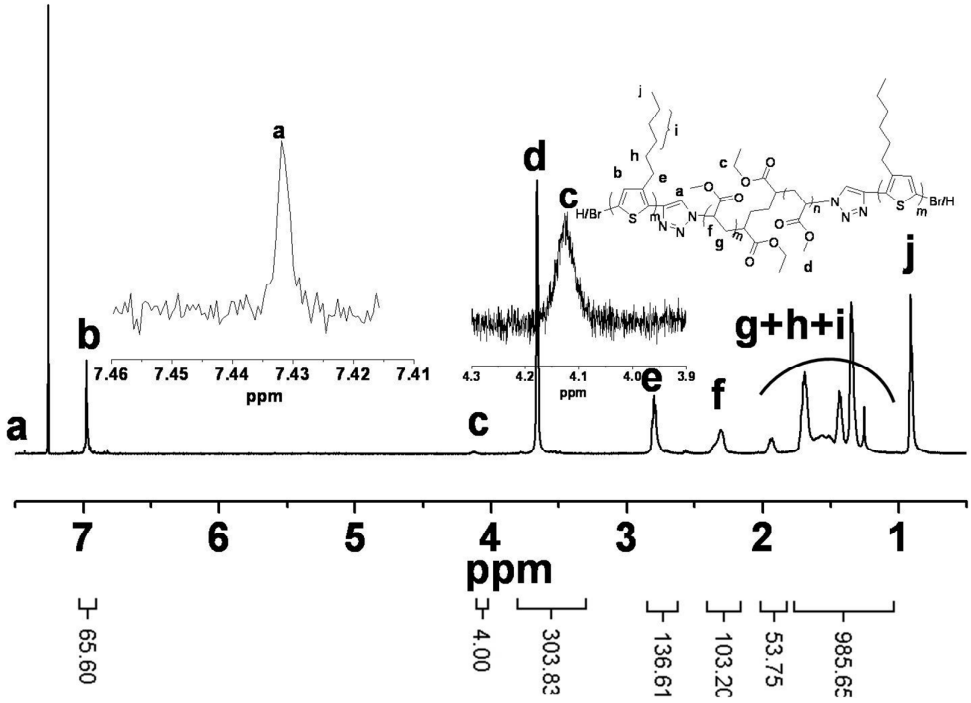

Figure 2. The HNMR spectrum of P3HT-*b*-PMA-*b*-P3HT triblock copolymer (P3).

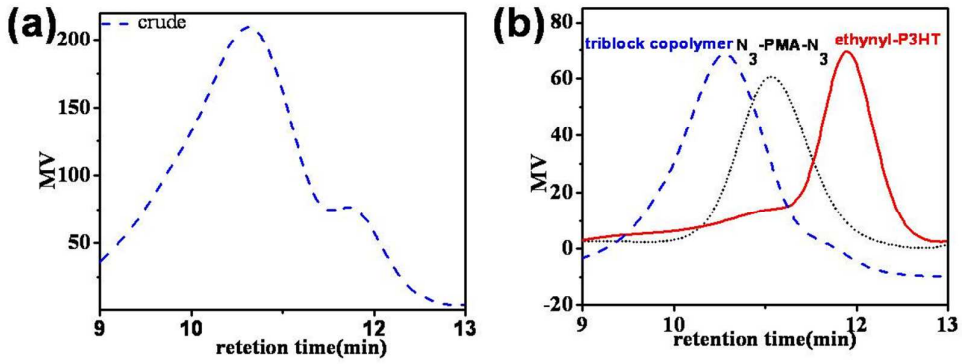

Figure 3. Representative GPC trace of the crude product (a, blue line) and highly purified triblock copolymers (b, blue line), poly(methylacrylate) homopolymer (b, black line) and P3HT homopolymer (b, red line).

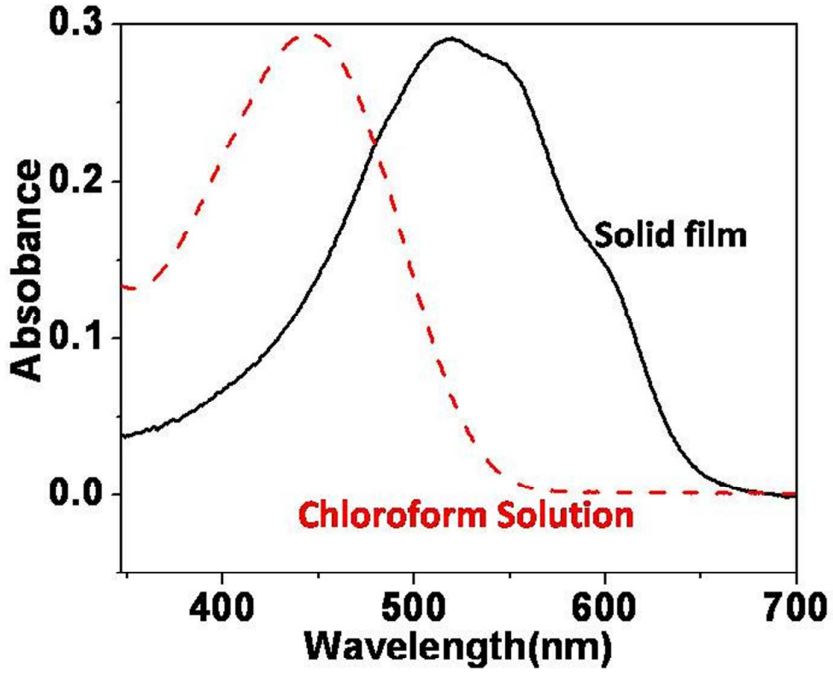

Figure 4. UV-vis absorption spectra of P3HT-*b*-PMA-*b*-P3HT in chloroform solution and in a thin film.

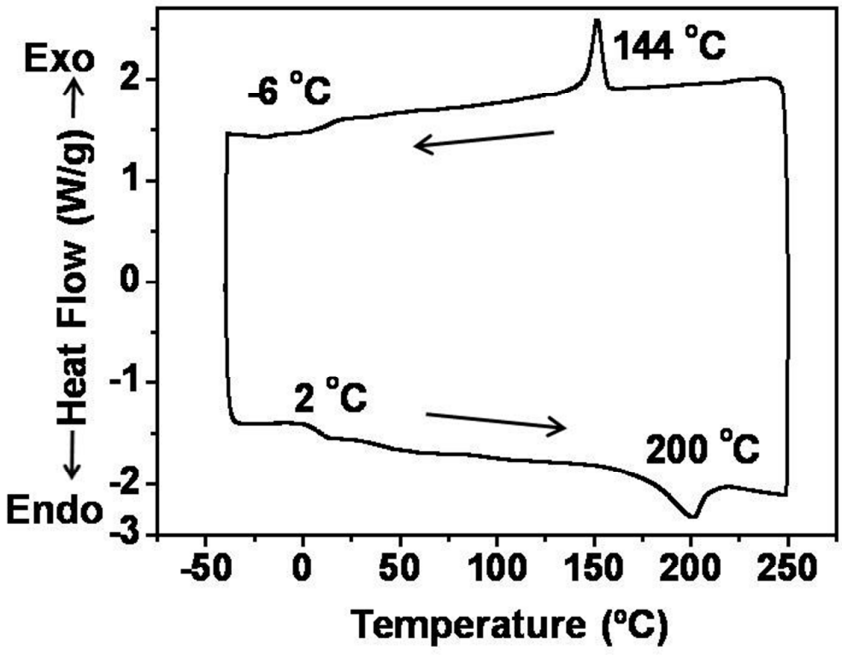

Figure 5. The DSC trace of P3HT-PMA-P3HT triblock copolymer.

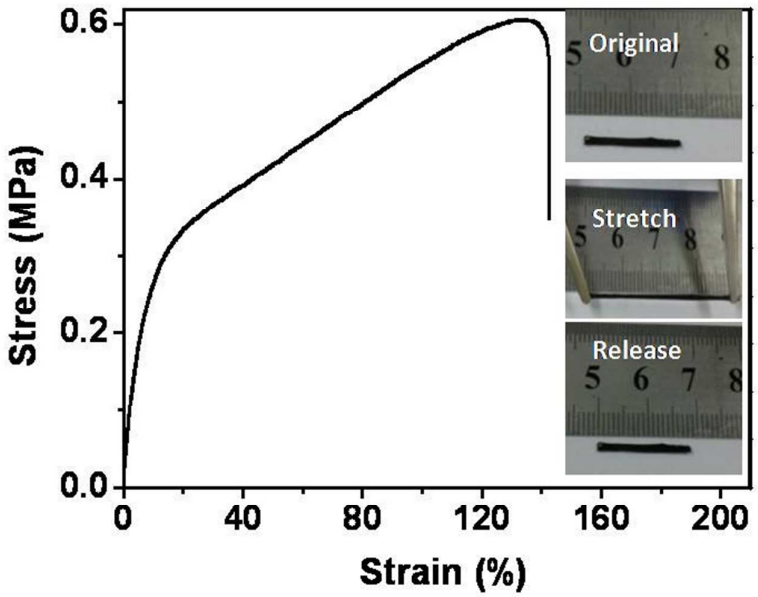

Figure 6. The strain–stress profile of P3HT-PMA-P3HT triblock copolymer.

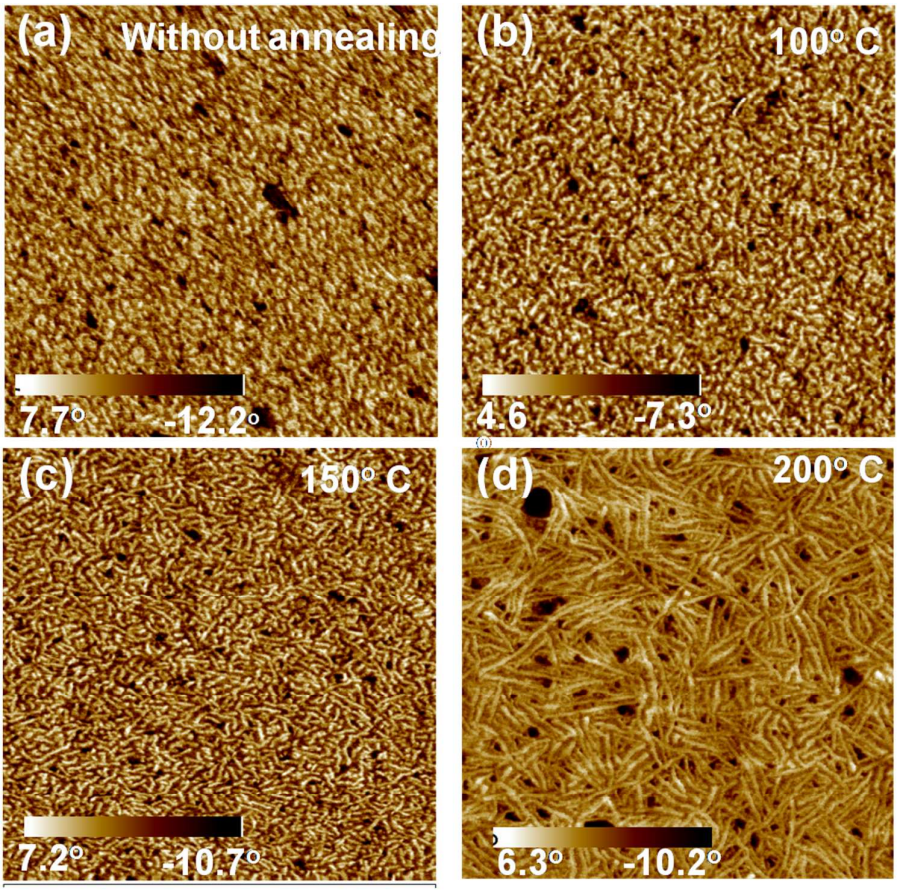

Figure 7. AFM topography images (a-d) of P3HT-PMA-P3HT at different annealing temperature.

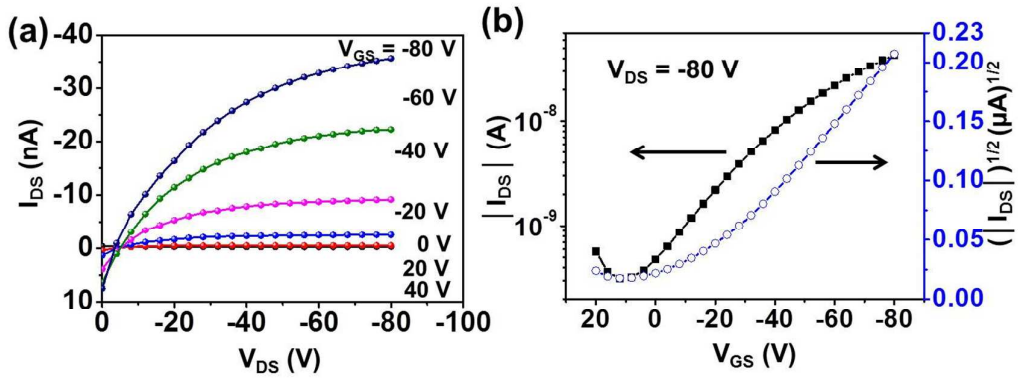

Figure 8. Field-effect characteristics of a top contact OFETs based on P4. (a) Output, and (b) transfer.

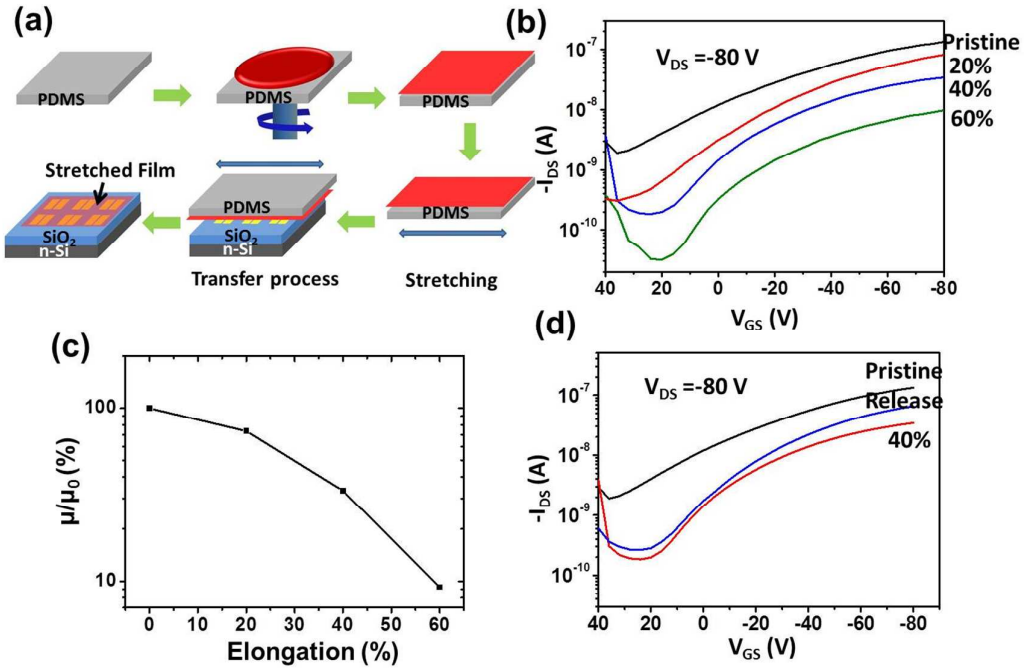

Figure 9. (a) Schematic illustration of the steps used to measure the mobility under stress. (b) Change of the transfer curves at different strains. (c) The corresponding change of mobility as a function of strains. (d) Change of the transfer curves during a stretching cycle at strain of 40%.

Graphical Abstract

An ABA Triblock Copolymer Strategy for Intrinsically Stretchable Semiconductor

Rui Peng,[a] Daqing Hu,[a] Mengjie Chen, [a] Bo Pang,[a] Guobing Zhang,[a] Xianghua Wang,[a] Hongbo Lu,[a,b] Kilwon Cho,[c] Longzhen Qiu[a,b]*

A novel semiconductor-rubber-semiconductor triblock copolymer has been designed and prepared according to the principle of thermoplastic elastomers(TPEs). It behaves as TPEs and exhibits good electrical properties.